Cancer Immunology Connect
ISSN: 3105-3629
2026, Article ID. 2026.0012, Cite as: https://doi.org/10.69709/TCTC.2026.199772

SCIFINITI PUBLISHING

Research Article

OPEN ACCESS

Association of 12q21.32 cn-LOH Affecting the *KITLG* p53 Response Element with Therapy Resistance in Acute Leukemia

Natalya Risinskaya[✉,1,*] **Sofia Starchenko**[✉,1] **Yulia Chabaeva**[✉,1] **Abdulpatakh Abdulpatakhov**[✉,1] **Ekaterina Kotova**[✉,1] **Valeriya Surimova**[✉,1] **Dmitry Bessmertnyy**[✉,1] **Anastasia Kashlakova**[✉,1] **Anastasia Vasileva**[✉,1] **Zalina Fidarova**[✉,1] **Olga Aleshina**[✉,1] **Anna Yushkova**[✉,1] **Olga Dubova**[✉,1] **Kseniya Nikiforova**[✉,1] **Nikolay Kapranov**[✉,1] **Irina Galtseva**[✉,1] **Alina Ponomareva**[✉,2] **Ilya Kanivets**[✉,2] **Sergey Korostelev**[✉,2] **Sergey Kulikov**[✉,1] **Elena Parovichnikova**[✉,1]

[1] National Medical Research Center for Hematology, 125167 Moscow, Russia
[2] Genomed Laboratory of Molecular Pathology, 115419 Moscow, Russia

Article History
Received: December 02, 2025 Accepted: February 18, 2026 Published: March 26, 2026

Abstract

Background: The tumor suppressor p53 is a key regulator of gene expression in cancer, functioning through binding to specific p53 response elements (REs). A functional SNP (rs4590952) is located within a p53 response element in the KITLG gene. **Aims**: This study aimed to precisely investigate the allelic variants of the SNP rs4590952 within patient groups with acute leukemia and to analyze their association with the disease and response to therapy. A specific objective was to determine the frequency and characteristics of regions of homozygosity encompassing the *KITLG* locus. **Methods:** The study cohort comprised 37 patients with Ph-negative B-ALL, 38 with T-ALL, and 35 with de novo intermediate-risk AML. A reference group of 200 healthy individuals without oncohematological disorders was included for comparison. Chromosomal microarray analysis (CMA) was performed using the CytoScan™ HT-CMA. Statistical analysis was performed using Python 3.12.4 and SAS 9.4. **Results:** The allele frequency (AF) of the G allele of rs4590952 was 0.785 in the reference group. Among patients, the AF was 0.833 in T-ALL, 0.757 in B-ALL, and 0.743 in AML. The frequency of copy-neutral loss of heterozygosity (cn-LOH) at 12q21.32, which results in the GG genotype, was significantly higher in the T-ALL group (45%) compared to the reference group (27%) (OR = 0.4; 95% CI: 0.2–0.9; $p = 0.02$). A significant association between MRD-positive status and cn-LOH KITLG was found specifically in the T-ALL group (OR = 11; 95% CI: 2–62; $p = 0.005$). Cn-LOH KITLG was also significantly associated with poor chemotherapy response in AML ($p = 0.01$). **Summary:** The GG genotype of the p53 response element in KITLG (rs4590952) frequently arises from acquired cn-LOH at 12q21.32, observed in 45% of T-ALL and 26–27% of other cases. This treatment-response marker, present regardless of leukemic status, warrants further validation in larger cohorts.

Keywords:
rs4590952; 12q21.32; Copy-Neutral Loss of Heterozygosity (cn-LOH); p53 response element–KITLG (p53 RE–KITLG); chemotherapy response; Minimal Residual Disease (MRD); T-Cell Acute Lymphoblastic Leukemia (T-ALL); B-Cell Acute Lymphoblastic Leukemia (B-ALL); Acute Myeloid Leukemia (AML)

1. Introduction

The tumor suppressor protein p53 is a central regulator of cellular defense against cancer, earning it the designation "the guardian of the genome." Its primary function is to serve as a sequence-specific transcription factor [1]. In response to cellular stresses such as DNA damage, oncogene activation, or hypoxia, p53 becomes stabi-

* **Corresponding Author:**
Natalya Risinskaya, National Medical Research Center for Hematology, 125167 Moscow, Russia, risinskaya.n@blood.ru

lized and activated. It subsequently binds to specific DNA sequences known as p53 response elements (p53 REs) [2]. These response elements have a consensus sequence of RRRCWWGYYY, followed by 0 to 13 random bases, and then another RRRCWWGYYY sequence (where R = A/G, W = A/T, Y = C/T) [3]. These response elements are typically located within the regulatory regions, such as promoters or enhancers, of target genes. Upon binding to its target response elements, p53 functions as a master transcriptional regulator, orchestrating a complex anti-cancer program by either activating or repressing specific genes.

Owing to its potent anti-proliferative effects, the p53 gene (TP53) is the most frequently mutated gene in human cancers. When p53 is inactivated, these critical protective pathways fail, allowing damaged cells to proliferate uncontrollably. One of the best-characterized p53 response elements in *KITLG* contains the single-nucleotide polymorphism rs4590952 (A>G), which has been shown to enhance p53 binding, increase *KITLG* expression, and potentially contribute to oncogenic effects. The *KITLG* gene (also known as Stem Cell Factor or Steel Factor), which encodes the ligand for the KIT receptor tyrosine kinase, is essential for critical physiological processes such as hematopoiesis, melanogenesis, gametogenesis, and mast cell function. However, this vital signaling pathway exhibits a dual nature, as its dysregulation through overexpression or constitutive activation can be co-opted in oncogenesis, thereby promoting tumor cell proliferation and survival, angiogenesis, and metastasis [4].

Consequently, the tight regulatory control of *KITLG* expression is paramount, as its loss can lead to significant oncogenic consequences. The contribution of the *KITLG* polymorphism rs4590952 to cancer risk is complex and appears to be context-dependent. One body of research has identified it as a key functional variant that enhances p53 binding, significantly upregulating *KITLG* expression and conferring one of the largest inherited risks for certain cancers, notably testicular cancer. This perspective is supported by evolutionary evidence of positive selection, indicating a past beneficial effect, and by the general rarity of such polymorphisms due to negative selection, highlighting their potential deleterious impact [5]. However, this conclusion is not universal. Contrary to the established mechanism, a focused study on breast cancer in a Chinese Han population found no significant association between rs4590952 and disease risk, even when stratified by hormone receptor status [6]. This discrepancy suggests that the oncogenic impact of this polymorphism may be highly cancer-type specific, indicating that heterogeneous mechanisms contribute to the etiology of different cancers and cautioning against broad generalizations of its risk profile.

The SNP rs4590952 is located at chr12:88,559,882 (GRCh38) within an intronic region of the *KITLG* gene. This polymorphism is characterized by a canonical allelic change of A > G, and its minor allele frequency demonstrates substantial variation across global populations. For instance, the frequency of the 'A' allele ranges from as low as 14.5% in a Northern Swedish cohort to over 43% in the PAGE_STUDY and nearly 48% in the TOMMO cohort, highlighting substantial inter-population diversity [7]. Despite its intronic location, this variant is of high functional significance, as it resides within a critical p53 transcription factor binding site, where the A > G change increases p53 binding affinity and modulates *KITLG* gene expression.

Building on prior data from pilot cohorts of patients with AML, B-ALL, and T-ALL, and leveraging chromosomal microarray analysis (CMA) based on single nucleotide polymorphism (SNP) arrays, this study aimed to investigate the allelic variants of rs4590952 (included in the CytoScan HD CMA panel as marker AX-17068144) within these patient groups. Special attention was paid to chromosomal events involving the *KITLG* locus. Key prognostic covariates (age, initial leukocyte count, cytogenetic/molecular risk, baseline MRD, and ELN risk in AML) were evaluated in our previous studies, with no association found with therapy response in the intermediate-prognosis groups of ALL and AML [8–11]. To establish the baseline frequency of KITLG RE allelic variants in the Russian population, a control cohort of individuals without a diagnosis of oncopathology who underwent genetic testing for family planning purposes was analyzed. The study aimed to assess the association between rs4590952 allelic variants and specific types of acute leukemia, as well as to investigate their potential relationship with therapy response.

2. Materials and Methods

2.1. Study Cohort

The study included a total of 110 patients with acute leukemia who were treated at the National Medical Research Center for Hematology. The cohort comprised the following: 37 patients with Philadelphia chromosome-negative B-cell Acute Lymphoblastic Leukemia (Ph-negative B-ALL), treated according to the RALL-2016m protocol (2019–2023) [ClinicalTrials.gov NCT06237192]. Male: Female ratio was 16:21. The median age was 36.5 years, ranging from 21 to 55 years. At presentation, the median leukocyte count was 8.23×10^9/L (range: 0.86–466.53), and the median percentage of blast cells in the

2026, Vol. 2, Article ID. 2026.0012
https://doi.org/10.69709/TCTC.2026.199772

bone marrow was 88% (range: 33.8–98). According to the EGIL and WHO classifications, the immunophenotypic distribution was as follows: B-I in 5 patients (13.5%), B-II in 30 patients (81.0%), B-III in 1 patient (2.7%), and B-IV in 0 patients (0%).

38 patients with Ph-negative T-cell Acute Lymphoblastic Leukemia (T-ALL), treated according to the RALL-2016m protocol (2017–2023) [ClinicalTrials.gov NCT06237192]. Male: Female ratio was 28:10 and a median age of 35.5 years (range: 19–53). The median leukocyte count at presentation was 46.18 $\times$ 10⁹/L, with a range of 0.95 to 445 $\times$ 10⁹/L. Bone marrow blast cell infiltration was high, with a median of 85.4% (range: 5.2–100). Immunophenotyping according to EGIL and WHO criteria identified the following subtypes: T-I in 5 patients (13.2%), T-II in 16 patients (42.1%), T-III in 14 patients (36.8%), and T-IV in 1 patient (2.6%). Additionally, two cases (5.7%) were classified as mixed-phenotype acute leukemia with T-myeloid features (MPAL T-myelo).

35 patients with de novo Acute Myeloid Leukemia (AML) of intermediate risk according to the ELN-2017 classification (2017–2024) [12]. [ClinicalTrials.gov NCT05339204]. Male: Female ratio was 11:24. The median age was 40 years, ranging from 19 to 62 years. At presentation, the median leukocyte count was 22 $\times$ 10^9/L (range: 1–254), and the median percentage of blast cells in the bone marrow was 78% (range: 10–94.4). For 9 AML patients with cn-LOH at 12q21.32, paired DNA samples from non-tumor tissue, including buccal epithelium, blood collected during remission, and mesenchymal stem cells, were subsequently analyzed. This analysis was specifically initiated to validate the somatic or germline origin of the cn-LOH after its initial discovery at the *KITLG* locus in tumor DNA.

The reference group included 200 healthy individuals without oncohematological disorders who underwent comparable CMA testing.

2.2. Cytogenetic and Molecular Diagnostics at Onset

At diagnosis, all patients underwent comprehensive immunophenotyping, cytogenetic, and molecular analysis of bone marrow samples. Conventional Cytogenetics: Bone marrow cells were analyzed using G-banding for karyotyping and Fluorescence In Situ Hybridization (FISH). All karyotype and FISH results were described according to the International System for Human Cytogenomic Nomenclature (ISCN) 2020 [13].

2.3. Minimal Residual Disease (MRD) Assessment

Minimal residual disease (MRD) was assessed in bone marrow samples by multiparameter flow cytometry (MFC), employing a combination of the "different from normal" (DfN) and leukemia-associated immunophenotype (LAIP) approaches. In patients with T-ALL, the flow cytometry panel for MRD assessment included CD99, CD7, CD3 (cytoplasmic/surface), CD5, CD45, CD8, CD34, CD56, and CD4 [14]. For B-ALL, the antibody panel included CD19, CD45, CD38, CD10, CD34, CD58, CD20, CD22, and CD24. In AML cases, MRD was assessed using panels of antibodies against the following antigens: CD15, CD38, CD371, CD34, CD117, CD33, CD13, CD99, CD14, CD123, CD11b, CD45RA, CD45, HLA-DR, CD16, and CD10. Additionally, one antibody associated with a patient-specific LAIP was included (e.g., CD2, CD4, CD5, CD7, CD11a, or CD56). Flow cytometry was performed on either a BD FACSCanto II (with 6-color panels before 2020) or a Beckman Coulter CytoFLEX (with 9–10 color panels after 2021). The primary endpoint was the achievement of MRD-negative status at the end of induction therapy.

2.4. Chromosomal Microarray Analysis (CMA)

Genomic DNA was isolated from diagnostic bone marrow aspirates. DNA was extracted using a standard phenol-chloroform method [14], quantified on a Qubit 4 fluorometer, and assessed for integrity (fragment length $\geq$ 10,000 bp). CMA was performed at the "Genomed" laboratory (Moscow, Russia) using the CytoScan™ HT array (Thermo Fisher Scientific, Waltham, MA, USA) according to the manufacturer's protocol. Tumor DNA (100–200 ng) was hybridized against reference male DNA. Scanning was performed on a GENOSCAN 3000 or similar platform. Raw data were processed and analyzed using Chromosome Analysis Suite (ChAS v.4.3.0.71) software (Thermo Fisher Scientific). The allelic variants of rs4590952 and chromosomal events affecting this SNP were analyzed (Figure 1).

2.5. Statistical Analysis

Categorical variables were summarized as frequencies. Differences in the distribution of categorical features between comparison groups were evaluated using Fisher's exact test or the chi-square test, as appropriate. All statistical analyses were performed using Python 3.12.4 and SAS software, version 9.4 (SAS Institute Inc., Cary, NC, USA).

2026, Vol. 2, Article ID. 2026.0012
https://doi.org/10.69709/TCTC.2026.199772

SCIFINITI PUBLISHING

Chromosome	Position	In Cytoregion	Markers CytoScan_HTCMA_96 dbSnp: 150 NetAffx: 36	BAF	Genotype Calls	LOH	Allele Difference	Copy Number State	Log2 Ratio
12	88,559,882	X	AX-170686144	0.9908	BB	1	-0.79966	2	-0.29273

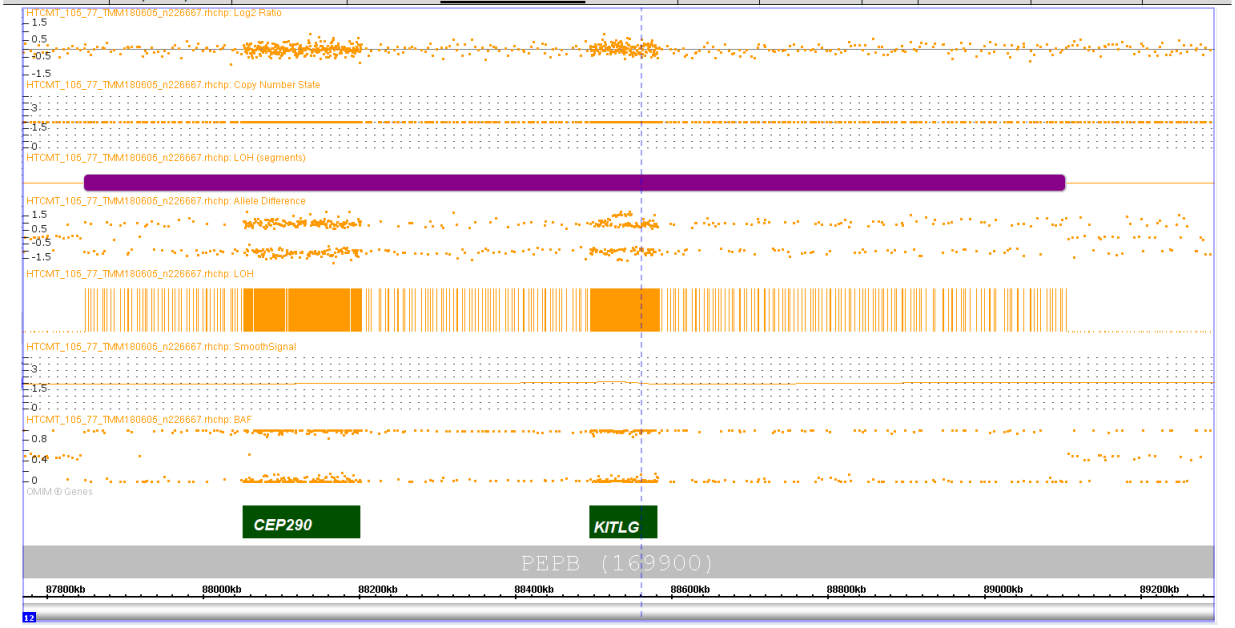

Figure 1: Analysis of the rs4590952 polymorphism in ChAS software (v.4.3.0.71). The region of interest on chromosome 12 is shown. The rs4590952 polymorphism (chr12:88559882 (GRCh38/hg38), CytoScan™ HT-CMA marker AX-17068144) is marked by the blue dashed line and is identified as having the BB (GG) allelic variant (panel above). An expanded view demonstrating that the *KITLG* gene is located within a region of loss of heterozygosity (LOH), approximately 1 megabase in size.

Generative AI tools, such as DeepSeek and Perplexity, were used for text editing, paraphrasing, and grammar checking when preparing the manuscript.

3. Results

The genotypic distribution within the reference cohort (n = 200) is summarized below. The homozygous A/A genotype was observed in 7 subjects (3.5%), one of whom exhibited a recorded cn-LOH. The heterozygous A/G genotype was found in 72 subjects (36%), and the homozygous G/G genotype was the most common, found in 121 subjects (60.5%). Notably, a cn-LOH spanning the *KITLG* gene was identified in 53 (43.8%) G/G homozygotes (Figure 2). The corresponding allele frequencies, derived from a total of 400 alleles, were 0.215 for allele A and 0.785 for allele G. The association between cn-LOH and demographic parameters such as gender and age was not revealed (Table 1).

In the T-ALL cohort (n = 38), the genotype distribution was: A/A in 3 patients (7.9%), A/G in 6 (15.7%), and G/G in 27 (71%). Cn-LOH covering the *KITLG* gene was detected in 17 (63%) of the G/G homozygotes. Additionally, two patients carried a duplication containing the *KITLG* gene, with allelic variants G/G/G and A/G/G. The overall allele frequency, including these duplications, was 0.166 for the A allele (13/78) and 0.833 for the G allele (65/78).

Table 1: Association between cn-LOH and demographics of healthy individuals (Gender and Age).

Parameters		Norm	cn-LOH	OR (95% CI)	p
Gender	Male	37	13	0.85 (0.41–1.74)	0.65
	Female	106	44		
Age	<45 y.o.	129	50	1.29 (0.49–3.38)	0.60
	≥45 y.o.	14	7		

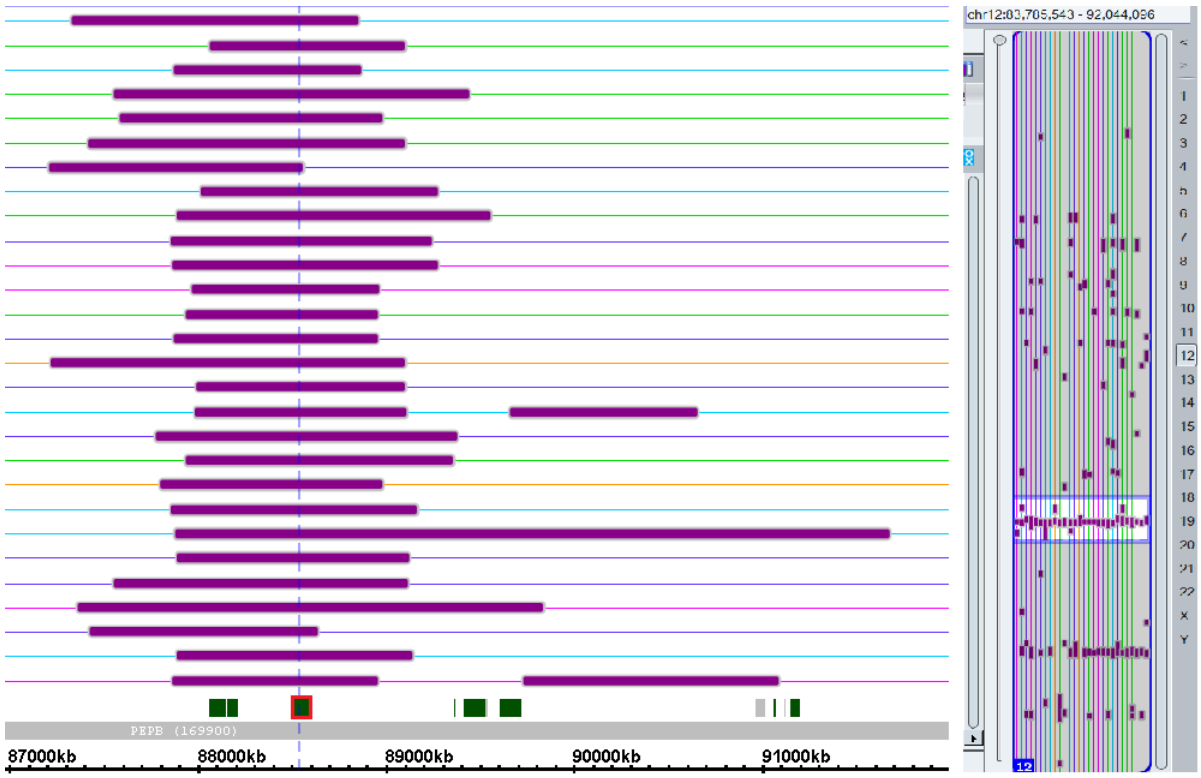

Figure 2: ChAS plot illustrating the sizes and positions of cn-LOH regions (shown in purple) on chromosome 12q21.32 in healthy individuals. The genomic position of the RE *KITLG* is indicated by a blue dashed vertical line.

Genotype analysis of the B-ALL cohort (n = 37) revealed an A/A genotype in 2 patients (5.4%), A/G in 14 (37.8%), and G/G in 21 (56.8%). Furthermore, cn-LOH at the *KITLG* locus was detected in 10 (47.6%) of the G/G homozygotes. The resultant overall allele frequencies were 0.243 for the A allele and 0.757 for the G allele.

In the AML cohort (n = 35), the genotype distribution was as follows: A/A in 1 patient (2.9%), A/G in 16 (45.7%), and G/G in 18 (51.4%). Cn-LOH spanning the *KITLG* locus was identified in 9 (50.0%) of the G/G homozygous patients. The overall allele frequency was 0.257 for the A allele (18/70) and 0.743 for the G allele (52/70). Deviation from the Hardy-Weinberg equilibrium was tested in each population. The results, including observed allele frequencies, chi-square (χ^2) statistics, and p-values, are presented in Table 2. Notably, significant deviation from HWE was observed only in the T-ALL cohort (p = 0.005), which also demonstrated the highest frequency of cn-LOH events in the 12q21.32 region. This concordance suggests tumor-specific selective pressure favoring homozygosity at this locus in T-cell leukemia.

Table 2: Hardy-Weinberg equilibrium analysis results.

Population	N	Allele Frequency (p = A, q = G)	χ^2	p	In HWE? (α = 0.05)
T-ALL	38	p = 0.166, q = 0.833	7.698	0.005	No
B-ALL	37	p = 0.243, q = 0.757	0.049	0.825	Yes
AML	35	p = 0.257, q = 0.743	3.117	0.077	Yes (Borderline)
Healthy	200	p = 0.215, q = 0.785	1.625	0.203	Yes

The distribution of allelic variants is shown in Figure 3. Comparison of allele genotypes between the acute leukemia groups and the reference group using the chi-square test revealed no statistically significant differences.

2026, Vol. 2, Article ID. 2026.0012
https://doi.org/10.69709/TCTC.2026.199772

Figure 3: Genotype distribution of the rs4590952 polymorphism across the study cohorts. The figure legend is displayed on the right, and the absolute counts for each genotype group are overlaid on the respective colored bars.

However, evaluation of the cn-LOH 12q21.32 frequency showed a statistically significant increase of this event in the T-ALL group (OR = 0.4; 95% CI: 0.2–0.9; p = 0.02). Consequently, the identified factor, rather than the allelic variants, was used to assess its association with therapy response.

A significant association between MRD+ status and cn-LOH *KITLG* was found specifically in the T-ALL group (OR = 11; 95% CI: 2–62; p = 0.005), unlike in B-ALL (Figure 4) or AML groups (Figure 5).

While no significant impact on outcome was observed in ALL cohorts, likely due to subsequent targeted therapy or HSCT according to RALL-2016m protocol, cn-LOH *KITLG* was significantly associated with poor chemotherapy response in AML (p = 0.01) (Figure 5).

CMA analysis of matched-pair DNA samples from non-tumor tissue revealed cn-LOH at 12q21.32 in 8 out of 9 AML patients with *KITLG* cn-LOH.

Analysis of 52 healthy individuals (26 with and 26 without cn-LOH *KITLG*) demonstrated a statistically significant increase in allelic imbalance at heterozygous SNP markers within the 2 Mbp region flanking rs4590952 (±1 Mbp) in the cn-LOH group (Mann-Whitney U test, p = 0.003) (Figure 6A,B and Figure 7).

Figure 6A shows a significant decrease in the number of heterozygous SNP markers with a BAF close to 0.5 and a concurrent significant increase in the number of heterozygous SNP markers with a BAF below 0.3 and above 0.7 compared to the data presented in Figure 6B. This is particularly notable given that a precise, patient-specific analysis of the cn-LOH region was not performed; instead, a common interval of 2 million base pairs centered on rs4590952 was applied to the entire cohort.

2026, Vol. 2, Article ID. 2026.0012
https://doi.org/10.69709/TCTC.2026.199772

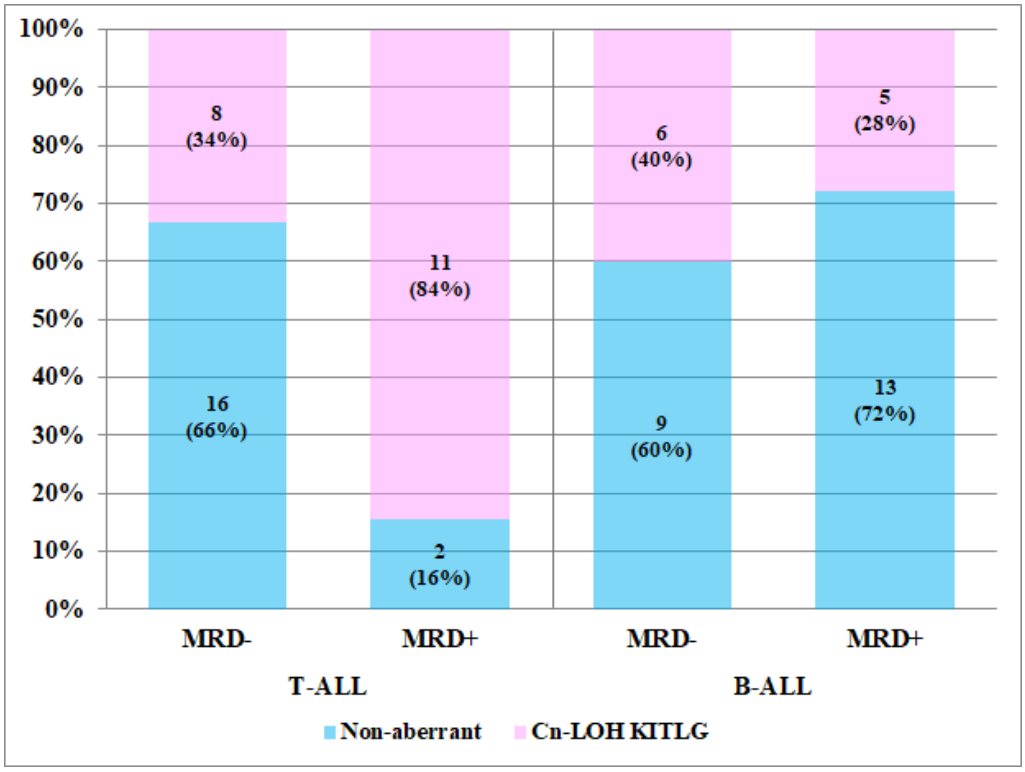

Figure 4: Distribution of *KITLG* cn-LOH in MRD-positive and MRD-negative T-ALL patients (One patient was excluded from the analysis because of early death; two patients with the AGG and GGG genotypes were MRD-positive, and all patients with the aberrant event were grouped into the cn-LOH *KITLG* group) and B-ALL patients (MRD status was not assessed in four patients).

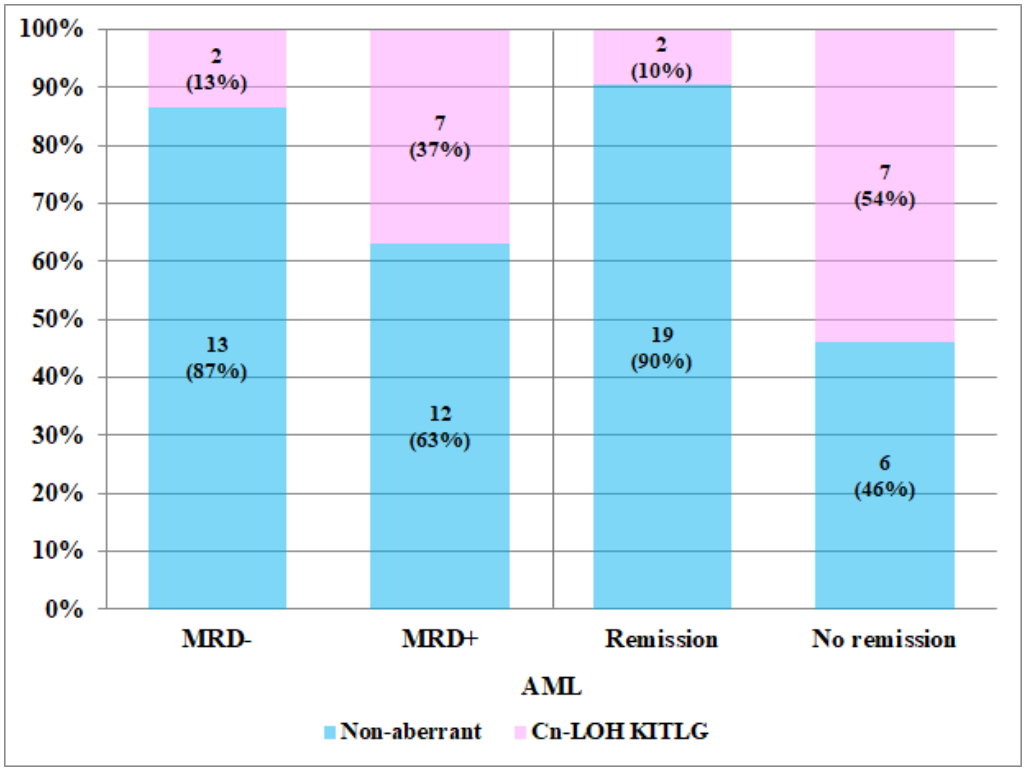

Figure 5: Distribution of *KITLG* cn-LOH in MRD-positive and MRD-negative AML patients (one patient was excluded from the analysis because of early death) and distribution according to chemotherapy response (right).

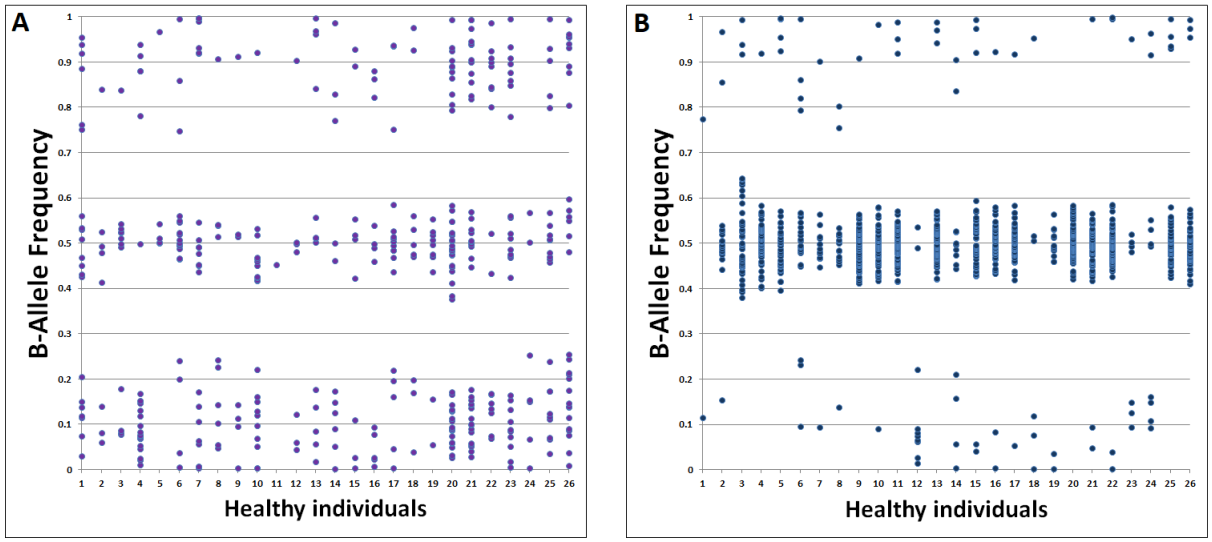

Figure 6: BAF distribution for heterozygous markers within ±1 Mbp of rs4590952 in cn-LOH positive individuals (**A**) and in cn-LOH negative individuals (**B**). Patient identifiers are plotted on the X-axis against B-allele frequency (BAF) values on the Y-axis. Heterozygous SNPs, as determined by CMA, are indicated by purple points.

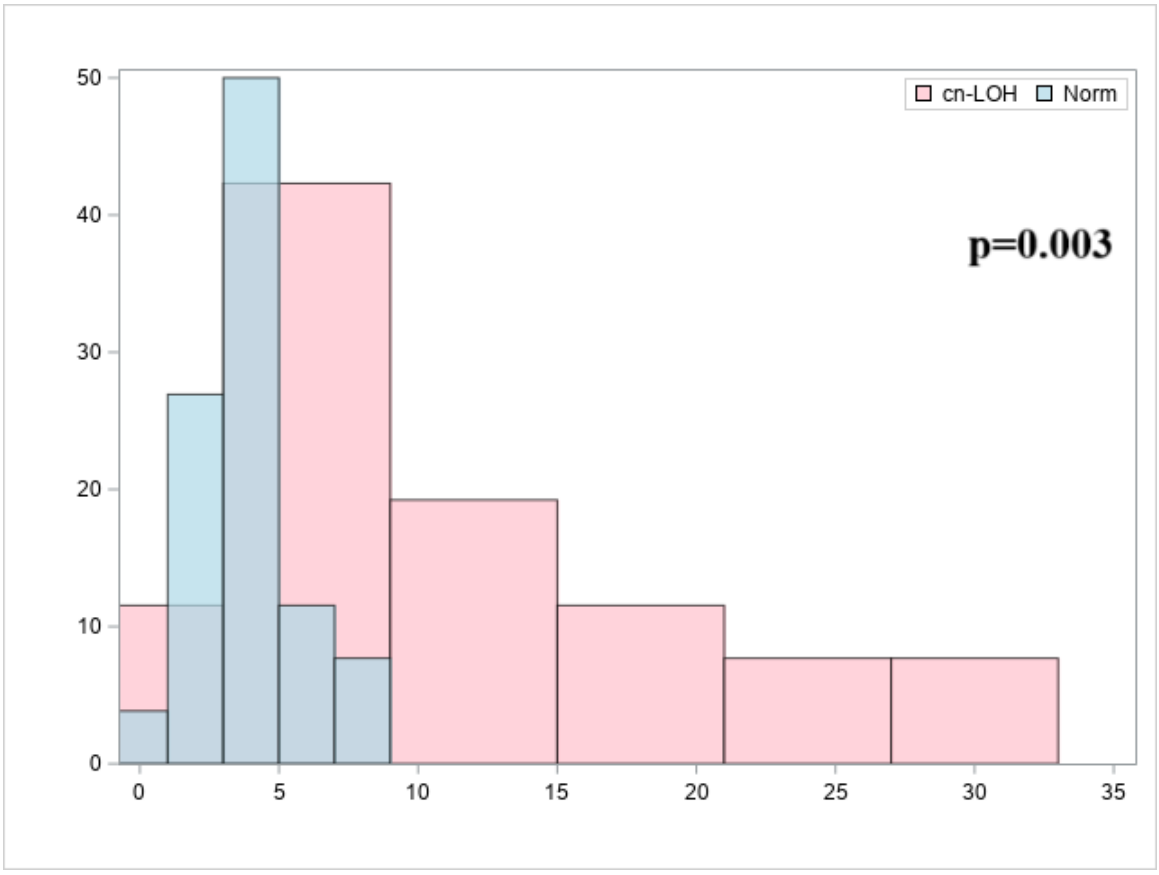

Figure 7: Graphical plot of the Mann-Whitney test. The X-axis shows the possible number of SNPs with allelic imbalance. The Y-axis shows the percentage of individuals with a specific number of SNPs with allelic imbalance. The blue color indicates the distribution of SNPs in the group with the normal 12q21.32 variant (ranging from 0 to 9 markers per person). The pink color indicates the distribution of SNPs in the group with the homozygosity/cn-LOH region at 12q21.32 (ranging from 0 to 33 markers per person).

2026, Vol. 2, Article ID. 2026.0012
https://doi.org/10.69709/TCTC.2026.199772

This graph provides visual support for the findings. The pink distribution (cn-LOH group) is shifted sharply to the right compared to the blue distribution (normal group). This means individuals in the cn-LOH group have a significantly higher number of SNPs with allelic imbalance. The difference in the range (0–9 vs. 0–33 markers per person) provides concrete, quantitative evidence of allelic imbalance in the cn-LOH group. The Mann-Whitney U test indicated that the difference between the two groups was statistically significant, suggesting that it is unlikely to have occurred by chance. In summary, this plot provides both visual and statistical evidence that the 12q21.32 region in the "pink" group exhibits a genetic profile characterized by high allelic imbalance, consistent with somatic cn-LOH rather than normal inherited homozygosity.

4. Discussion

The *KITLG* gene encoding stem cell factor (SCF) is an evolutionarily significant locus that has undergone a hard selective sweep in human populations over the past millennia, which is associated with adaptations in skin pigmentation and other features [15]. The *KITLG* locus has undergone strong positive selection throughout human history and also demonstrates remarkable stability, with its adaptive haplotype maintaining a high frequency and persistent selection signal over thousands of years, despite substantial demographic changes [15]. This evolutionary stability underscores the fundamental importance of the gene and explains why its aberrant regulation is frequently observed in pathologies, including malignant neoplasms. The extended homozygosity encompassing the *KITLG* gene, as identified in our analysis, aligns with established signatures of recent positive selection in Eurasian populations, a pattern previously linked to adaptations such as skin pigmentation and winter climate by Yang et al. This provides a crucial evolutionary backdrop, demonstrating that the *KITLG* locus is under strong germline selection [16].

The critical importance of the *KITLG* signaling pathway is normally emphasized by its key role in regeneration processes. As shown in the study of bone regeneration, *KITLG*, expressed by specialized endothelial cells, is the central organizer of the osteovascular niche, recruiting precursors and directing osteogenic differentiation [17]. This physiological function of *KITLG* (SCF) signaling as a niche organizer and survival factor for stem/progenitor cells helps explain why aberrant activation of this pathway is often observed in oncologic contexts, where the tumor "captures" these normal support mechanisms.

To investigate the potential clinical significance of a specific p53 response element in the *KITLG* gene, the study focused on its well-established role as a direct transcriptional target of p53. The genome-wide mapping study by Tebaldi et al. [18] aimed to rank p53 response elements (REs) based on their transactivation potential. Within this research, the gene *KITLG* was robustly validated as a direct p53 transcriptional target. This conclusion is supported by multiple lines of evidence: the p53 retriever algorithm predicted a high-ranking p53 binding site in the KITLG promoter, independent ChIP-seq data confirmed direct p53 binding, and microarray analysis demonstrated increased KITLG mRNA levels following p53 activation by doxorubicin. Furthermore, subsequent qPCR validation in isogenic cell lines with differing p53 status confirmed that *KITLG* induction was strictly p53-dependent. The study, therefore, definitively classifies *KITLG* as a direct p53 target gene, linking p53 pathway activation to the regulation of this key player in cell cycle control and tumor progression. Findings in leukemia are complemented by data from solid tumors, where high *KITLG* expression has been shown to be a hallmark of type A and AB thymomas, promoting oncogenesis through MAPK pathway activation [19].

This parallel underscore the broader role of *KITLG* as a potential diagnostic biomarker and therapeutic target across multiple malignancies. The controversial role of *KITLG* as an oncogene or suppressor is further illustrated by its expression in breast cancer: it is highly expressed and plays an unfavorable role in the HR+ subtype [20], but is expressed at low levels and associated with poor outcomes in TNBC [21]. In colorectal cancer, for example, increased *KITLG* levels expressed by fibroblasts and tumor endothelium correlate with the activation of infiltrating mast cells and, paradoxically, with improved patient survival, emphasizing its potential protective immunomodulatory role in this context [22]. This contrast illustrates the critical importance of the cellular source of *KITLG* and the tumor type in determining the final effect of its signal. In addition to its immunomodulatory functions, KITLG can also act as a classical oncogenic driver. In nasopharyngeal carcinoma (NPC), its overexpression in tumor cells directly correlates with lymph node metastasis and poor prognosis, and *KITLG* suppression inhibits invasion and metastasis, probably through activation of the JAK/STAT pathway [23]. Independent confirmation of the central role of KITLG in NPC pathogenesis was obtained through co-expression network analysis (WGCNA), which identified this gene as a key hub associated with histological grade and tumor stage. Interestingly, this analysis also linked the KITLG-containing module to the p53 pathway and cell cycle regulation [24], consistent with evidence that its expression is regulated via the p53 response element. These findings indicate that tumor cells can autonomously exploit the KITLG-cKIT pathway to enhance their aggressiveness.

Stimulation of tumor cell proliferation through KITLG is often mediated by activation of the MAPK/ERK pathway. In multiple myeloma (MM), this activation occurs through a unique mechanism: the oncogenic splicing factor DAZAP1 directly regulates alternative splicing of *KITLG* mRNA, ultimately leading to ERK phosphorylation and accelerated tumor growth [25]. The role of alternative splicing as a critical regulator of *KITLG's* oncogenic function has been convincingly demonstrated in lung adenocarcinoma. The tumor suppressor, lncRNA SPAT, by inhibiting the SF1 splicing factor, shifts *KITLG* splicing towards the formation of the less active isoform *KITLG*-201, while suppressing the production of the oncogenic isoform *KITLG*-205. Increased levels of *KITLG*-205 directly correlate with activation of the ERK/MAPK pathway, increased cell migration, and poor patient prognosis [26]. This mechanism highlights that therapeutic strategies targeting the KITLG pathway may include modulating its splicing to suppress specific, most aggressive isoforms. Thus, the KITLG-ERK pathway represents a common endpoint for diverse regulatory aberrations.

The study of Zhang et al. [27] demonstrates a critical interaction between germline genetic variation in the p53 pathway and somatic TP53 mutations, collectively influencing cancer risk, progression, and therapy response.

The oncogenic role of *KITLG* (SCF) is convincingly confirmed not only in acute leukemias, but also in chronic lymphoproliferative diseases. In chronic lymphocytic leukemia (CLL), leukemic cells predominantly overexpress the SCF membrane isoform. This overexpression is an independent unfavorable prognostic factor correlating with a short time to start therapy and overall survival, and also serves as a key regulator of interactions with the microenvironment. Notably, SCF levels decrease in response to the BTK inhibitor ibrutinib, a standard therapy for CLL, indicating the involvement of this pathway in the drug's mechanism of action and highlighting KITLG as a potential target for therapeutic intervention in this disease [28]. In AML, single-cell RNA sequencing (scRNA-seq) revealed that low expression of the key stromal factor KITLG in bone marrow aspirates is an independent prognostic marker associated with significantly improved overall survival [29,30]. The role of cn-LOH 12q in the progression of leukemia is confirmed in the work of Sinclair et al. In B-ALL with iAMP21, the cn-LOH 12q event, which results in homozygous mutations in SH2B3, constitutes an unfavorable prognostic factor [31], consistent with findings on the significance of cn-LOH 12q21.32 in AML and T-ALL.

Therefore, strategies aimed at suppressing this pathway, whether by direct inhibition or indirect regulation of its expression, are of therapeutic interest. For example, in glioblastoma, one mechanism underlying the antitumor effect of MSC therapy is the downregulation of the *KITLG* gene [32]. Precision medicine algorithms are starting to consider *KITLG* as a predictor biomarker. For example, the DDPP algorithm for predicting the outcome of therapy identified the *KIT-KITLG* pair as the optimal two-gene signature correlating with the duration of progressive survival (PFS) in patients receiving the antiangiogenic drug axitinib [33]. These findings indicate that the transcriptomic status of the *KITLG* pathway may serve as a tool for patient stratification and the selection of optimal targeted therapies. Importantly, chemotherapy itself can enhance the pathogenic effects of KITLG. Sublethal doses of doxorubicin induce the release of extracellular vesicles enriched in *KITLG* from melanoma cells, which directly impair cardiomyocyte mitochondrial function, revealing a novel mechanism of tumor-mediated cardiotoxicity [34].

The universal role of *KITLG* in stromal cell pathology is also confirmed in a non-oncological context. In age-related osteoporosis, it has been identified as one of the key genes whose expression changes in aging BMSCs within the miRNA-mRNA regulatory network affecting the PI3K-Akt pathway [35]. This indicates that abnormalities in the regulation of *KITLG* in the stromal niche can lead not only to malignant transformation (leukemia) but also to degenerative processes associated with aging. Similarly, in renal fibrosis associated with diabetic nephropathy, *KITLG* functions as a key mediator of tissue damage [36]. The diagnostic potential of alterations at the *KITLG* locus is not limited to genomic variations. Thus, in ovarian seminoma, analysis of KITLG promoter methylation in cfDNA from liquid biopsies (blood plasma) is being explored as a non-invasive biomarker approach [37], illustrating the progression from studying gene function to developing practical diagnostic applications.

The significance of *KITLG* as a cancer-associated gene is evident even in veterinary medicine: germline copy number variations (CNVs) of this gene are an established predisposition factor for digital squamous cell carcinoma in Schnauzer dogs [38].

Our study, focused on assessing copy number variations (CNV) and cn-LOH at the *KITLG* locus, employed CMA based on high-resolution SNP microarrays This technology is fundamentally based on the hybridization of fragmented, fluorescently labeled sample DNA to specific oligonucleotide probes immobilized on a chip. Subsequent analysis of signal intensities and genotype calls (B-allele frequency) enables the simultaneous detection of a broad spectrum of genomic alterations, ranging from large copy number variations (CNVs) to subtle copy-neutral events [39–41]. This comprehensive genomic profiling capability was pivotal for our investigation. The SNP

2026, Vol. 2, Article ID. 2026.0012
https://doi.org/10.69709/TCTC.2026.199772

array platform offers dual analytical capabilities: first, it enables high-throughput genotyping of the rs4590952 SNP across the entire patient and control cohort. Secondly, and crucially, it enabled a detailed analysis of the molecular genotype across the 12q21.32 locus. This specific feature, the ability to detect regions of homozygosity through shifts in B-allele frequency without corresponding changes in copy number, enabled the unambiguous identification of acquired cn-LOH, a key finding of the study.

A combined analytical approach is essential to distinguish between evolutionarily selected germline ROH (regions of homozygosity) and acquired somatic cn-LOH in the study. Population genetics provides the initial filter: the frequency and genomic architecture of the homozygous segment can be indicative. Long, frequent ROH tracts are often signatures of identity-by-descent due to shared ancestry [42]. However, conclusive evidence for a postzygotic, somatic event comes from the detection of allelic imbalance at heterozygous sites within the region. The presence of heterozygous SNPs with allelic ratios systematically deviating from the expected 0.5, as observed in data from healthy individuals with cn-LOH, is a hallmark of somatic genetic alteration [43,44]. This mosaicism, detectable even in non-malignant cells, confirms the event as acquired rather than inherited. Therefore, integrating population-based allele frequencies with high-resolution analysis of allelic ratios using techniques such as microarrays or next-generation sequencing enables robust discrimination of cn-LOH from ROH [45]. The study of Kim & Suyama [46] provides critical population-level context, revealing that cn-LOH is a frequent and intrinsic genetic phenomenon in healthy individuals, with an average of 40.7 events per genome. A majority (65%) of these events were classified as gonosomal mosaicism, present in both germline and somatic cells. Importantly, their work suggests that the occurrence of cn-LOH is influenced by genomic architecture, with a tendency to increase in GC-rich regions and on chromosomes where homologs are in closer spatial proximity.

This study investigated the nature of the 12q21.32 homozygosity region. Specifically, is it a result of evolutionary selection for a single allele in the population, a classic homozygote inheriting identical alleles from both parents, or is it a somatic event that occurred during early post-zygotic stages? A direct answer to this question would have been provided by genotyping the parents of the individuals included in the study. However, we had neither the opportunity nor the objective to do so.

It was hypothesized that in cases of post-zygotic cn-LOH, which implies mosaicism and the concurrent existence of a cell population retaining the allele, there would be an increase in the number of heterozygous markers exhibiting allelic imbalance. In other words, an increased number of AG markers with B-allele frequencies (BAF) below 0.3 and above 0.7 would be expected. Conversely, in the case of an inherited homozygosity region, the number of heterozygous markers with allelic imbalance would not exceed this same parameter in the group where no loss of heterozygosity was observed. To minimize technical batch effects when comparing the two groups, the B-allele frequency (BAF) of heterozygous SNP markers from the CytoScan™ HT-CMA panel was analyzed exclusively for samples processed within a single CMA batch (a run of 96 samples). Consequently, the cohort was structured to include 26 samples with 12q21.32 loss of heterozygosity (27% of 96) and 26 samples without it. Our study, which identified a high frequency of 12q21.32 cn-LOH, aligns with this ACMG technical standard. Our conclusion that this homozygosity is not due to consanguinity but is a recurrent somatic event (postzygotic cn-LOH) is fully consistent with the interpretation principles outlined by the ACMG. The significant allelic imbalance observed at heterozygous SNP markers within the locus provides direct evidence against inherited ROH and confirms the somatic origin of cn-LOH, in accordance with ACMG guidelines for accurate diagnosis [47].

Mentions of 12q21.32 cn-LOH are scarce in the literature because, in CMA diagnostics, loss-of-heterozygosity events smaller than 3 million base pairs are typically disregarded due to their frequent occurrence in the healthy genome. However, Wen et al. identified a recurrent ROH region at 12q21.3 with a frequency greater than 1% in a cohort of 958 cases with normal karyotype and aCGH results, included in the study over the four years from 2014 to 2017; this cohort consisted of 142 parental, 500 postnatal/pediatric, 195 prenatal CVS, and 121 prenatal AF cases [48]. It is hypothesized that this genomic feature may not have phenotypic consequences in healthy individuals, but in patients with acute leukemias, it could be indirectly associated with poorer responses to chemotherapy.

In conclusion, the data suggest that acquired 12q21.32 cn-LOH is likely a more important determinant of chemotherapy response than the germline allelic variants of the p53 response element in *KITLG*. The population frequency of the G allele falls within the range established for other populations and shows no association with leukemia. It can be inferred that the rs4590952 G allele, particularly the GG genotype, is not causative but rather serves as a marker for another factor or event within the 12q21.32 cn-LOH region, with the emergence of the homozygous p53 response element genotype occurring in close proximity. However, we are aware of the limitations

of our work. Firstly, the small sample size of patients made it difficult to perform statistical analysis and prevented us from conducting a reliable multivariate analysis that included standard prognostic covariates. Secondly, the retrospective nature of the study prevented us from analyzing functional data, such as *KITLG* expression, KIT pathway activation, and downstream signaling pathways, after identifying aberrations affecting *KITLG*.

This study is a pilot exploratory investigation aimed at identifying novel potential risk factors. Future validation of 12q21.32 homozygosity/cn-LOH phenomenon in larger, prospective acute leukemia cohorts, with mandatory profiling of matched tumor-free samples, could establish it as a novel biomarker to guide the inclusion of targeted agents into first-line therapy for patients carrying this specific genetic marker.

5. Conclusions

The population frequency of the rs4590952 G allele (controls 0.785; T-ALL 0.833; B-ALL 0.757; AML 0.743) falls within the range reported for other populations and, in the patient, cohorts studied, shows no significant association with acute leukemia ($p > 0.05$). The GG genotype frequently arises from acquired cn-LOH at 12q21.32, observed in 45% of T-ALL and 26–27% of other cases ($p = 0.02$). This pattern is consistent with a recurrent postzygotic event rather than evolutionarily selected germline homozygosity, as indicated by significant allelic imbalance at heterozygous SNPs within the region. Critically, 12q21.32 cn-LOH is associated with MRD positivity in T-ALL and poor chemotherapy response in AML. This treatment-response marker, present irrespective of leukemic status, warrants further validation in expanded cohorts.

List of Abbreviations

ACMG	American College of Medical Genetics and Genomics
AF	Allele Frequency
AML	Acute Myeloid Leukemia
BAF	B-Allele Frequency
B-ALL	B-cell Acute Lymphoblastic Leukemia
ChAS	Chromosome Analysis Suite
CMA	Chromosomal Microarray Analysis
cn-LOH	Copy-Neutral Loss of Heterozygosity
CNV	Copy Number Variations
ELN	European Leukemia Net
FISH	Fluorescence In Situ Hybridization
HWE	Hardy-Weinberg Equilibrium
MAF	Minor Allele Frequency
Mbp	Mega Base Pairs
MPAL T-myelo	Mixed-Phenotype Acute Leukemia with T-myeloid Features
MRD	Minimal Residual Disease
mRNA	Messenger RNA
qPCR	Quantitative PCR
RE	Response Element
ROH	Runs/Regions of Homozygosity
SNP	Single Nucleotide Polymorphism
T-ALL	T-cell Acute Lymphoblastic Leukemia

Author Contributions

Conceptualization: N.R.; methodology: S.K. (Sergey Kulikov); validation: N.R., S.S., D.B., A.A. and E.K.; formal analysis: S.S., V.S. and Y.C.; investigation: K.N., O.D., A.Y., N.K., A.P., I.K. and S.K.(Sergey Korostelev); resources: E.K., A.A., A.V., Z.F., O.A., A.K., A.V. and I.G.; writing—original draft preparation: N.R. and S.S.; writing—review and editing: S.K. (Sergey Kulikov); visualization: S.S. and Y.C.; supervision: S.K. (Sergey Kulikov); project administration: E.P.; funding acquisition: N.R. and D.B. All authors have read and agreed to the published version of the manuscript.

Availability of Data and Materials

The data used in this study are available at: https://doi.org/10.6084/m9.figshare.30739889, accessed on 19 January 2026.

Ethical Committee Approval and Consent to Participate

The study was approved by the Ethics Committee of the National Medical Research Center for Hematology (protocol #175/25, 25 October 2023) and the Local Ethical Committee of Genomed Laboratory of Molecular Pathology (protocol #G2024/12, 12 October 2024). Informed consent was taken from all patients and healthy participants.

Human Rights Statement

The study was conducted in accordance with the Declaration of Helsinki.

Conflicts of Interest

The authors declare no conflicts of interest.

Funding

The funding for this research was provided by the Russian Science Foundation (RSF) project No. 23-25-00490 https://www.rscf.ru/en/project/23-25-00490/ (accessed on 25 November 2025). CMA for the AML patient cohort was

performed with support from the National Hematological Society (NHS), Moscow, Russia.

Acknowledgments

Declared none.

AI Declaration

The authors acknowledge the use of DeepSeek and Perplexity to improve the English language, including grammar and readability, during manuscript preparation. All scientific content, data analysis, and conclusions were generated and verified by the authors, who take full responsibility for the final text.

References

[1] Fischer, M.; Sammons, M.A. Determinants of p53 DNA Binding, Gene Regulation, and Cell Fate Decisions. *Cell Death Differ.* **2024**, *31*, 836–843. [CrossRef] [PubMed] [PubMed Central]

[2] Sammons, M.A.; Nguyen, T.T.; McDade, S.S.; Fischer, M. Tumor Suppressor p53: From Engaging DNA to Target Gene Regulation. *Nucleic Acids Res.* **2020**, *48*, 8848–8869. [CrossRef] [PubMed] [PubMed Central]

[3] Farooq, Z.; Wani, S.; Ragunathrao, V.A.B.; Kochhar, R.; Anwar, M. *P53 Tumor Suppressor: Functional Regulation and Role in Gene Therapy*; p53-A Guardian of the Genome and Beyond; IntechOpen: London, UK, 2022. [CrossRef]

[4] Wang, X.; Ren, H.; Zhao, T.; Chen, J.; Sun, W.; Sun, Y.; Ma, W.; Wang, J.; Gao, C.; Gao, S.; et al. Stem Cell Factor is a Novel Independent Prognostic Biomarker for Hepatocellular Carcinoma after Curative Resection. *Carcinogenesis* **2014**, *35*, 2283–2290. [CrossRef] [PubMed]

[5] Zeron-Medina, J.; Wang, X.; Repapi, E.; Campbell, M.R.; Su, D.; Castro-Giner, F.; Davies, B.; Peterse, E.F.; Sacilotto, N.; Walker, G.J.; et al. A Polymorphic p53 Response Element in KIT Ligand Influences Cancer Risk and Has Undergone Natural Selection. *Cell* **2013**, *155*, 410–422. [CrossRef] [PubMed] [PubMed Central]

[6] Chen, W.; Li, J.; Liu, C.; Chen, X.; Zhu, Y.; Yang, Y.; Gong, Y.; Wang, T.; Miao, X.; Nie, X. A Functional p53 Responsive Polymorphism in KITLG, rs4590952, Does Not Affect the Risk of Breast Cancer. *Sci. Rep.* **2014**, *4*, 6371. [CrossRef] [PubMed] [PubMed Central]

[7] National Center for Biotechnology Information (NCBI). dbSNP Short Genetic Variations. Available online: https://www.ncbi.nlm.nih.gov/snp/?term=rs4590952+KITLGrs4590952 (accessed on 2 December 2025).

[8] Risinskaya, N.; Gladysheva, M.; Abdulpatakhov, A.; Chabaeva, Y.; Surimova, V.; Aleshina, O.; Yushkova, A.; Dubova, O.; Kapranov, N.; Galtseva, I.; et al. DNA Copy Number Alterations and Copy Neutral Loss of Heterozygosity in Adult Ph-Negative Acute B-Lymphoblastic Leukemia: Focus on the Genes Involved. *Int. J. Mol. Sci.* **2023**, *24*, 17602. [CrossRef]

[9] Risinskaya, N.; Abdulpatakhov, A.; Chabaeva, Y.; Aleshina, O.; Gladysheva, M.; Nikulina, E.; Bolshakov, I.; Yushkova, A.; Dubova, O.; Vasileva, A.; et al. Biallelic Loss of 7q34 (TRB) and 9p21.3 (CDKN2A/2B) in Adult Ph-Negative Acute T-Lymphoblastic Leukemia. *Int. J. Mol. Sci.* **2024**, *25*, 10482. [CrossRef]

[10] Surimova, V.; Risinskaya, N.; Kotova, E.; Abdulpatakhov, A.; Vasileva, A.; Chabaeva, Y.; Starchenko, S.; Aleshina, O.; Kapranov, N.; Galtseva, I.; et al. PSG and Other Candidate Genes as Potential Biomarkers of Therapy Resistance in B-ALL: Insights from Chromosomal Microarray Analysis and Machine Learning. *Int. J. Mol. Sci.* **2025**, *26*, 7437. [CrossRef]

[11] Bessmertnyy, D.K.; Starchenko, S.E.; Risinskaya, N.V.; Kulikov, S.M.; Chabaeva, U.A.; Surimova, V.A.; Ponamoreva, A.S.; Kanivets, I.V.; Fidarova, Z.T.; Lukianova, I.A.; et al. Structural Aberrations of Genes Associated with Leukemogenesis in Patients with Acute Myeloid Leukemia of Intermediate Prognosis. *Russ. J. Hematol. Transfusiology (Gematol. I Transfuziol.)* **2025**, *70*, 465–477. (in Russian). [CrossRef]

[12] Döhner, H.; Estey, E.; Grimwade, D.; Amadori, S.; Appelbaum, F.R.; Büchner, T.; Dombret, H.; Ebert, B.L.; Fenaux, P.; Larson, R.A.; et al. Diagnosis and Management of AML in Adults: 2017 ELN Recommendations from an International Expert Panel. *Blood* **2017**, *129*, 424–447. [CrossRef] [PubMed] [PubMed Central]

[13] McGowan-Jordan, J.; Ros, J. *ISCN 2020: An International System for Human Cytogenomic Nomenclature*, 1st ed.; S. Karger AG: Basel, Switzerland, 2020. [CrossRef]

[14] Barton, D.E. DNA Prep for Eukaryotic Cells (Macrophages) [Electronic Forum Post]. BioNet Methods and Reagents. July 1995. Available online: http://www.bio.net/bionet/mm/methods-and-reagents/1995-July/031231.html (accessed on 18 June 2025).

[15] Harris, M.; Mo, Z.; Siepel, A.; Garud, N. The Persistence and Loss of Hard Selective Sweeps Amid Ancient Human Admixture. *bioRxiv* **2025**. [CrossRef] [PubMed] [PubMed Central]

[16] Yang, Z.; Shi, H.; Ma, P.; Zhao, S.; Kong, Q.; Bian, T.; Gong, C.; Zhao, Q.I.; Liu, Y.; Qi, X.; et al. Darwinian Positive Selection on the Pleiotropic Effects of KITLG Explain Skin Pigmentation and Winter Temperature Adaptation in Eurasians. *Mol. Biology Evol.* **2018**, *35*, 2272–2283. [CrossRef]

[17] Li, X.; Kim, H.D.; Luo, A.C.; Gong, L.; Zhu, Y.; Lee, C.N.; Hong, X.; Sudduth, C.L.; Ad, M.; An, Y.H.; et al. Human Bone-Derived Endothelial Cells Mediate Bone Regeneration via Distinct Expression of

KIT Ligand. *Adv. Sci.* **2025**, *12*, e14194. [CrossRef] [PubMed] [PubMed Central]

[18] Tebaldi, T.; Zaccara, S.; Alessandrini, F.; Bisio, A.; Ciribilli, Y.; Inga, A. Whole-Genome Cartography of p53 Response Elements Ranked on Transactivation Potential. *BMC Genom.* **2015**, *16*, 464. [CrossRef] [PubMed] [PubMed Central]

[19] Yang, Z.; Liu, S.; Wang, Y.; Chen, Y.; Zhang, P.; Liu, Y.; Zhang, H.; Zhang, P.; Tao, Z.; Xiong, K. High Expression of KITLG Is a New Hallmark Activating the MAPK Pathway in Type A and AB Thymoma. *Thorac. Cancer* **2020**, *11*, 1944–1954. [CrossRef] [PubMed] [PubMed Central]

[20] Yang, Z.; Chen, H.; Yin, S.; Mo, H.; Chai, F.; Luo, P.; Li, Y.; Ma, L.; Yi, Z.; Sun, Y.; et al. PGR-KITLG Signaling Drives a Tumor-Mast Cell Regulatory Feedback to Modulate Apoptosis of Breast Cancer Cells. *Cancer Lett.* **2024**, *589*, 216795. [CrossRef] [PubMed]

[21] Qin, L.; Li, Y.; Huang, Y.; Tang, C.; Yang, W.; Tang, Y.; Qiu, C.; Mao, M.; Li, J. Exploring the Biological Behavior and Underlying Mechanism of KITLG in Triple-Negative Breast Cancer. *J. Cancer* **2024**, *15*, 764–775. [CrossRef] [PubMed] [PubMed Central]

[22] Xie, Z.; Niu, L.; Zheng, G.; Du, K.; Dai, S.; Li, R.; Dan, H.; Duan, L.; Wu, H.; Ren, G.; et al. Single-Cell Analysis Unveils Activation of Mast Cells in Colorectal Cancer Microenvironment. *Cell Biosci.* **2023**, *13*, 217. [CrossRef] [PubMed] [PubMed Central]

[23] Ling, J.; Zhang, L.; Chang, A.; Huang, Y.; Ren, J.; Zhao, H.; Zhuo, X. Overexpression of KITLG Predicts Unfavorable Clinical Outcomes and Promotes Lymph Node Metastasis via the JAK/STAT Pathway in Nasopharyngeal Carcinoma. *Lab. Investig.* **2022**, *102*, 1257–1267. [CrossRef] [PubMed]

[24] Pan, X.; Liu, J.H. Identification of Four Key Biomarkers and Small Molecule Drugs in Nasopharyngeal Carcinoma by Weighted Gene Co-Expression Network Analysis. *Bioengineered* **2021**, *12*, 3647–3661. [CrossRef] [PubMed] [PubMed Central]

[25] Zhou, Y.; Huangfu, S.; Li, M.; Tang, C.; Qian, J.; Guo, M.; Zhou, Z.; Yang, Y.; Gu, C. DAZAP1 Facilitates the Alternative Splicing of KITLG to Promote Multiple Myeloma Cell Proliferation via ERK Signaling Pathway. *Aging* **2022**, *14*, 7972–7985. [CrossRef] [PubMed] [PubMed Central]

[26] Ma, Y.; Zhou, X.; Yu, M.; Cheng, X.; Yang, J.; Ren, J.; Zheng, C.; Li, J.; Qian, X.; Yi, J.; et al. SPAT Inhibits LUAD Metastasis by Targeting SF1-Mediated Splicing. *Cell Death Dis.* **2025**, *16*, 598. [CrossRef] [PubMed] [PubMed Central]

[27] Zhang, P.; Kitchen-Smith, I.; Xiong, L.; Stracquadanio, G.; Brown, K.; Richter, P.H.; Wallace, M.D.; Bond, E.; Sahgal, N.; Moore, S.; et al. Germline and Somatic Genetic Variants in the p53 Pathway Interact to Affect Cancer Risk, Progression, and Drug Response. *Cancer Res.* **2021**, *81*, 1667–1680. [CrossRef]

[28] Gavriilidis, G.I.; Ntoufa, S.; Papakonstantinou, N.; Kotta, K.; Koletsa, T.; Chartomatsidou, E.; Moysiadis, T.; Stavroyianni, N.; Anagnostopoulos, A.; Papadaki, E.; et al. Stem Cell Factor Is Implicated in Microenvironmental Interactions and Cellular Dynamics of Chronic Lymphocytic Leukemia. *Haematologica* **2021**, *106*, 692–700. [CrossRef] [PubMed] [PubMed Central]

[29] Zhou, J.; Chng, W.J. Unveiling Novel Insights in Acute Myeloid Leukemia through Single-Cell RNA Sequencing. *Front. Oncol.* **2024**, *14*, 1365330. [CrossRef] [PubMed] [PubMed Central]

[30] Chen, L.; Pronk, E.; Van Dijk, C.; Bian, Y.; Feyen, J.; Van Tienhoven, T.; Yildirim, M.; Pisterzi, P.; De Jong, M.M.E.; Bastidas, A.; et al. A Single-Cell Taxonomy Predicts Inflammatory Niche Remodeling to Drive Tissue Failure and Outcome in Human AML. *Blood Cancer Discov.* **2023**, *4*, 394–417. [CrossRef] [PubMed] [PubMed Central]

[31] Sinclair, P.B.; Ryan, S.; Bashton, M.; Hollern, S.; Hanna, R.; Case, M.; Schwalbe, E.C.; Schwab, C.J.; Cranston, R.E.; Young, B.D.; et al. SH2B3 Inactivation through CN-LOH 12q Is Uniquely Associated with B-Cell Precursor ALL with iAMP21 or Other Chromosome 21 Gain. *Leukemia* **2019**, *33*, 1881–1894. [CrossRef] [PubMed] [PubMed Central]

[32] Aslam, N.; Abusharieh, E.; Abuarqoub, D.; Ali, D.; Al-Hattab, D.; Wehaibi, S.; Al-Kurdi, B.; Jamali, F.; Alshaer, W.; Jafar, H.; et al. Anti-Oncogenic Activities Exhibited by Paracrine Factors of MSCs Can Be Mediated by Modulation of KITLG and DKK1 Genes in Glioma SCs in Vitro. *Mol. Ther. Oncolytics* **2020**, *20*, 147–165. [CrossRef] [PubMed] [PubMed Central]

[33] Lazar, V.; Magidi, S.; Girard, N.; Savignoni, A.; Martini, J.F.; Massimini, G.; Bresson, C.; Berger, R.; Onn, A.; Raynaud, J.; et al. Digital Display Precision Predictor: The Prototype of a Global Biomarker Model to Guide Treatments with Targeted Therapy and Predict Progression-Free Survival. *NPJ Precis. Oncol.* **2021**, *5*, 33. [CrossRef] [PubMed] [PubMed Central]

[34] Fernández-Fonseca, L.F.; Novoa-Herrán, S.; Umaña-Pérez, A.; Gómez-Grosso, L.A. Sublethal Doxorubicin Promotes Extracellular Vesicle Biogenesis in A375 Melanoma Cells: Implications for Vesicle-Loaded TGF-β-Mediated Cancer Progression and Cardiovascular Pathophysiology. *Int. J. Mol. Sci.* **2025**, *26*, 8524. [CrossRef] [PubMed] [PubMed Central]

[35] Gao, M.D.; Wang, X.J.; Li, P.B.; Dong, Q.Q.; Tian, L.M. A Novel Molecular Regulatory Network in Bone Marrow Mesenchymal Stem Cells for Age-Related Osteoporosis. *Clin. Endocrinol.* **2025**, *102*, 635–646. [CrossRef] [PubMed]

[36] Huang, J.C.; Chen, S.C.; Chang, W.A.; Hung, W.W.; Wu, P.H.; Wu, L.Y.; Chang, J.M.; Hsu, Y.L.; Tsai, Y.C. KITLG Promotes Glomerular Endothelial Cell Injury in Diabetic Nephropathy by an Autocrine Ef-

fect. *Int. J. Mol. Sci.* **2022**, *23*, 11723. [CrossRef] [PubMed] [PubMed Central]

[37] Raos, D.; Oršolić, D.; Mašić, S.; Tomić, M.; Krasić, J.; Tomašković, I.; Gabaj, N.N.; Gelo, N.; Kaštelan, Ž.; Kuliš, T.; et al. CfDNA Methylation in Liquid Biopsies as Potential Testicular Seminoma Biomarker. *Epigenomics* **2022**, *14*, 1493–1507. [CrossRef] [PubMed]

[38] Aupperle-Lellbach, H.; Heidrich, D.; Kehl, A.; Conrad, D.; Brockmann, M.; Törner, K.; Beitzinger, C.; Müller, T. KITLG Copy Number Germline Variations in Schnauzer Breeds and Their Relevance in Digital Squamous Cell Carcinoma in Black Giant Schnauzers. *Vet. Sci.* **2023**, *10*, 147. [CrossRef] [PubMed] [PubMed Central]

[39] Bumgarner, R. Overview of DNA Microarrays: Types, Applications, and Their Future Chapter 22:Unit 22.1. *Curr. Protoc. Mol. Biol.* **2013**, 22. [CrossRef] [PubMed]

[40] Heinrichs, S.; Li, C.; Look, A.T. SNP Array Analysis in Hematologic Malignancies: Avoiding False Discoveries. *Blood* **2010**, *115*, 4157–4161. [CrossRef] [PubMed] [PubMed Central]

[41] Govindarajan, R.; Duraiyan, J.; Kaliyappan, K.; Palanisamy, M. Microarray and Its Applications. *J. Pharm. Bioallied Sci.* **2012**, *4*, S310–S312. [CrossRef] [PubMed] [PubMed Central]

[42] Pemberton, T.J.; Absher, D.; Feldman, M.W.; Myers, R.M.; Rosenberg, N.A.; Li, J.Z. Genomic Patterns of Homozygosity in Worldwide Human Populations. *Am. J. Hum. Genet.* **2012**, *91*, 275–292. [CrossRef] [PubMed] [PubMed Central]

[43] Laurie, C.C.; Laurie, C.A.; Rice, K.; Doheny, K.F.; Zelnick, L.R.; McHugh, C.P.; Ling, H.; Hetrick, K.N.; Pugh, E.W.; Amos, C.; et al. Detectable Clonal Mosaicism from Birth to Old Age and Its Relationship to Cancer. *Nat. Genet.* **2012**, *44*, 642–650. [CrossRef] [PubMed] [PubMed Central]

[44] Jacobs, K.B.; Yeager, M.; Zhou, W.; Wacholder, S.; Wang, Z.; Rodriguez-Santiago, B.; Hutchinson, A.; Deng, X.; Liu, C.; Horner, M.J.; et al. Detectable Clonal Mosaicism and Its Relationship to Aging and Cancer. *Nat. Genet.* **2012**, *44*, 651–658. [CrossRef] [PubMed] [PubMed Central]

[45] Conlin, L.K.; Thiel, B.D.; Bonnemann, C.G.; Medne, L.; Ernst, L.M.; Zackai, E.H.; Deardorff, M.A.; Krantz, I.D.; Hakonarson, H.; Spinner, N.B. Mechanisms of Mosaicism, Chimerism and Uniparental Disomy Identified by Single Nucleotide Polymorphism Array Analysis. *Hum. Mol. Genet.* **2010**, *19*, 1263–1275. [CrossRef] [PubMed] [PubMed Central]

[46] Kim, H.; Suyama, M. Genome-Wide Identification of Copy Neutral Loss of Heterozygosity Reveals Its Possible Association with Spatial Positioning of Chromosomes. *Human Mol. Genet.* **2023**, *32*, 1175–1183. [CrossRef]

[47] Gonzales, P.R.; Andersen, E.F.; Brown, T.R.; Horner, V.L.; Horwitz, J.; Rehder, C.W.; Rudy, N.L.; Robin, N.H.; Thorland, E.C. Interpretation and Reporting of Large Regions of Homozygosity and Suspected Consanguinity/Uniparental Disomy, 2021 Revision: A Technical Standard of the American College of Medical Genetics and Genomics (ACMG). *Genet. Med.* **2022**, *24*, 255–261. [CrossRef] [PubMed]

[48] Wen, J.; Comerford, K.; Xu, Z.; Wu, W.; Amato, K.; Grommisch, B.; DiAdamo, A.; Xu, F.; Chai, H.; Li, P. Analytical Validation and Chromosomal Distribution of Regions of Homozygosity by Oligonucleotide Array Comparative Genomic Hybridization from Normal Prenatal and Postnatal Case Series. *Mol. Cytogenet.* **2019**, *12*, 12. [CrossRef] [PubMed]